MOLECULAR ONCOLOGY 7 (2013) 884–894

available at www.sciencedirect.com

SciVerse ScienceDirect

www.elsevier.com/locate/molonc

MicroRNA-9 enhances migration and invasion through KLF17 in hepatocellular carcinoma

Zhao Sun[a,1], Qin Han[b,1], Na Zhou[a], Shihua Wang[a], Shan Lu[c], Chunmei Bai[a,*], Robert Chunhua Zhao[b,d,**]

[a]Department of Oncology, Peking Union Medical College Hospital, Chinese Academy of Medical Sciences and Peking Union Medical College, Beijing 100730, People's Republic of China
[b]Center of Excellence in Tissue Engineering, Institute of Basic Medical Sciences and School of Basic Medicine, Chinese Academy of Medical Sciences and Peking Union Medical College, Beijing, People's Republic of China
[c]China National Center for Biotechnology Development, People's Republic of China
[d]Peking Union Medical College Hospital, Beijing, People's Republic of China

ARTICLE INFO

Article history:
Received 24 March 2013
Received in revised form
17 April 2013
Accepted 18 April 2013
Available online 25 April 2013

Keywords:
Hepatocellular carcinoma
Invasion
KLF-17
microRNA-9

ABSTRACT

Metastasis is one of the hallmarks of cancer malignancy that usually causes more detrimental effects than a primary tumor. Many microRNAs were reported to be involved in the process of tumor metastasis. Hep11 and Hep12 cells were derived from primary and recurrence (intrahepatic metastatic) sites of hepatocellular carcinoma (HCC), respectively. Hep12 exhibited a higher invasive and migratory potential than Hep11. There was also a significantly higher expression of miR-9 in Hep12 cells than in Hep11 cells. Further studies in HCC cell lines demonstrated that miR-9 could promote tumor cell migration and invasion. In addition, miR-9 downregulated KLF17 protein expression by targeting the 3′UTR region of the KLF17 gene directly. As a transcription factor, KLF17 directly acted on the promoters of EMT-related genes (ZO-1, Vimentin and Fibronectin (FN)) in HCC cell lines. Therefore, we conclude that miR-9 may possibly promote HCC migration and invasion through regulation of KLF17.

1. Introduction

It has been well established that the development of hepatocellular carcinoma (HCC) is associated with Hepatitis B virus (HBV) infection, Hepatitis C virus (HCV) infection and alcohol abuse. Although attempts to prevent HCC have already focused on these risk factors, the incidence of HCC is still high. In men, it is the fifth most commonly diagnosed cancer but the second leading cause of cancer death worldwide. In women, it is the seventh most frequently diagnosed cancer and the sixth leading cause of cancer death. The regions of high incidence include Eastern and Southeastern Asia, as well as Middle and Western Africa. Approximately 700,000 new cases of HCC are diagnosed worldwide every year, half

Abbreviations: HCC, hepatocellular carcinoma; HBV, Hepatitis B virus; EMT, epithelial mesenchymal transition; FBS, fetal calf serum; qRT-PCR, quantitative reverse transcription polymerase chain reaction; FN, fibronectin; WT, wild type; MT, mutant type; CHIP, chromatin immunoprecipitation; HNSCC, head and neck squamous cell carcinoma; Vim, vimentin; E-ca, E-cadherin; KLF17, Krüppel-like factor 17.

* *Corresponding author*. Tel.: +86 10 69158934.
** *Corresponding author*. Center of Excellence in Tissue Engineering, Institute of Basic Medical Sciences and School of Basic Medicine, Chinese Academy of Medical Sciences and Peking Union Medical College, Beijing, People's Republic of China. Tel./fax: +86 10 65125311.
E-mail addresses: baichunmei1964@yahoo.com.cn (R.C. Bai), chunhuaz@public.tpt.tj.cn (R.C. Zhao).
[1] Both authors contributed equally to this work.

1574-7891/$ – see front matter © 2013 Federation of European Biochemical Societies. Published by Elsevier B.V. All rights reserved.
http://dx.doi.org/10.1016/j.molonc.2013.04.007

of which are from China (Ferlay et al., 2010; Jemal et al., 2011). The high incidence of HCC in China is mainly attributed to the prevalence of chronic HBV infection (Ferlay et al., 2010; Jemal et al., 2011).

Currently, one of the obstacles in HCC treatment is the high rate of tumor relapse and metastasis. Therefore, inhibition of tumor invasion and metastasis would be a novel therapeutic strategy for HCC. Epithelial mesenchymal transition (EMT) plays a crucial role in tumor cell invasion and migration in many cancers, including HCC (Lin et al., 2012; Oishi et al., 2012; Wen et al., 2012). In this complex process, epithelial cells lose their basic characteristics. Such changes include the loss of apical-basal polarity, the disruption of cell–cell tight junctions and anchoring junctions, and the breakdown of desmosomes and keratin filaments. EMT contributes to the aggressive dissemination of carcinoma cells by allowing the cells to penetrate the basement membrane and subsequently invade the lymphatics and blood vessels. Hep11 and Hep12 are two cell lines that were previously established by primary culture from the same patient (Xu et al., 2010a,b). Hep11 cells, with obvious epithelial-like traits, were acquired after the patient's first radical surgery for primary HCC, when no metastasis was found. In contrast, Hep12 cells were acquired from a surgically resected tumor that relapsed after failed chemotherapy and radiotherapy, and these cells possessed mesenchymal-like characteristics with enhanced migratory and invasive abilities. In this study, we compared miRNA expression in these two cell lines using the miRNA microarray platform and observed that, intriguingly, the expression level of miR-9 in Hep12 cells was nearly a thousand fold higher than in Hep11 cells. This result was consistent with previous studies that showed miR-9 was highly expressed in metastatic HCC (Budhu et al., 2008; Tan et al., 2010). Clinical research about correlations between miR-9 and HCC progression/relapse has been reported (Budhu et al., 2008), but the molecular mechanisms governing miR-9 in HCC remain largely unknown. It has been reported that downregulation of KLF17 could promote breast cancer cell migration and invasion (Gumireddy et al., 2009), and reduced expression of KLF17 was correlated with tumor progression and poor prognosis in lung adenocarcinoma (Cai et al., 2012). In addition, analysis of relationship between KLF17 expression and the clinicopathological features of HCC in 60 patients also showed downregulated KLF17 expression was associated with tumor invasion and poor prognosis in hepatocellular carcinoma (Liu et al., 2013). As miRNAs exert functions through post transcriptional regulation of their target genes, we employed bioinformatics analysis which identified KLF17 as a miR-9 putative target gene. Therefore, we hypothesized that miR-9 may be involved in EMT and metastasis of HCC via the regulation of KLF17 expression.

2. Methods

2.1. Tumor cell culture

The human carcinoma cell lines HepG2 (human hepatic carcinoma) and SMMC7721 (human hepatic carcinoma) were purchased from Cell Resource Center, IBMS, CAMS/PUMC). They were maintained in DMEM medium (Gibco, Paisley, UK) supplemented with 10% fetal calf serum (FCS, Gibco, Paisley, UK) in humidified 5% CO2/95% atmosphere at 37 °C. Hep11 and Hep12 cells, which were established by primary culture from the same patient, were kind gifts from Dr. Wang Y; Hep11 was derived from the primary tumor, and Hep12 was derived from the relapsed tumor. Hep11 and Hep12 were cultured in RPMI-1640 medium (Gibco, Paisley, UK) supplemented with 20% of the patient's autologous serum as described previously (Xu et al., 2010a,b).

2.2. MicroRNA microarray analysis

Microarray assay and data analysis were performed using a service provider (LC Sciences). miRNA profiling was performed by high-throughput quantitative qRT-PCR using the TaqMan® Array Human MicroRNA Cards V3.0 (Applied Biosystems) following the manufacturer's instructions. Ten nanograms of total RNA were used for each reaction. PCRs were repeated at least twice, and the mean relative expression level was calculated. The U6 was used for data normalization (Applied Biosystems). Experiments were performed in triplicate.

2.3. miRNA and siRNA transfection

The synthetic miR-9 mimic (forward, 5′-UCUUUGGUUAUCUAGCUGUAUGA-3′; reverse, 5′-AUACAGCUAGAUAACCAAAGAUU-3′), miR-9 inhibitor (5′-UCAUACAGCUAGAUAACCAAAGA′-3′), mimic control (forward, 5′-UUCUCCGAACGUGUCACGUTT-3′; reverse, 5′-ACGUGACACGUUCGGAGAATT-3′) and inhibitor control (5′-UUGUACUACACAAAAGUACUG-3′) were purchased from GenePharma (GenePharma Inc., Shanghai, China). The siRNA for Klf17 was synthesized (GenePharma, Inc., Shanghai, China) to target 5′-CGACAGTACCTTCTGACGAAAC-3′(Gumireddy et al., 2009). The nucleotide sequences were delivered into human HCC cell lines by Amaxa Nucleofector® following the manufacturer's instructions. Briefly, cell pellets were collected by 90 × g centrifugation at room temperature for 10 min and resuspended in 100 μl of Nucleofector Solution to a final concentration of 1×10^6 cells/100 μl. Each 100 μl sample was transferred into an Amaxa-certified cuvette and underwent nucleofection using the appropriate Nucleofector program. The program for transfecting HepG2 and SMMC7721 was T028, and that for Hep12 was U008. After nucleofection, each sample was immediately transferred from the cuvette to a culture plate in 2 ml of medium (Li et al., 2011a,b).

2.4. RNA reversed transcription and qRT-PCR

Total RNA was extracted using the Trizol total RNA isolation reagent (Invitrogen) and purified with the Column DNA Erasol kit (TIANGEN, Beijing, China) according to the manufacturers' instructions. mRNA levels were assessed with qRT-PCR using SYBR Green I (TaKaRa, Dalian, China). The gene expression level was normalized to the endogenous reference gene *GAPDH*. The experiments were performed in triplicate. The primers for qRT-PCR are listed in Suppl. Table 1. The primers for miR-9 and U6 were purchased from QIAGEN. Reverse transcription of miRNAs was performed with a miScript Reverse Transcription Kit (QIAGEN, Duesseldorf,

Germany). The expression of mature miRNAs was determined using miRNA-specific quantitative qRT-PCR (TaKaRa, Dalian, China). The expression levels were normalized to the U6 endogenous control and measured by the comparative Ct ($\triangle\triangle$Ct) method.

2.5. Western blot analysis

After washing twice with PBS, cells were lysed in ice-cold Radio Immunoprecipitation Assay (RIPA) lysis buffer (Beyotime, Nanjing, China) and manually scraped from culture plates. Proteins were separated on 10% sodium dodecyl sulfate–polyacrylamide gel electrophoresis (SDS-PAGE) gels, electroblotted onto a polyvinylidene difluoride (PVDF) membrane and incubated with anti-KLF17 antibody (1/1000; Sigma, St Louis, USA), anti-ZO-1 antibody (1/1000; Santa Cruz Biotechnology, Santa Cruz, CA), anti-E-cadherin antibody (1/1000; R&D, Minneapolis, MN, USA), anti-β-catenin antibody (1/1000; Santa Cruz Biotechnology, Santa Cruz, CA), anti-Fibronectin antibody (1/1000; Santa Cruz Biotechnology, Santa Cruz, CA), anti-Vimentin antibody (1/1000; Santa Cruz Biotechnology, Santa Cruz, CA), anti-ID-1 antibody (1/1000; Santa Cruz Biotechnology, Santa Cruz, CA) or anti-GAPDH antibody (1/2000; Santa Cruz Biotechnology, Santa Cruz, CA), followed by incubation with a secondary anti-rabbit or anti-mouse horseradish peroxidase-conjugated antibody (Zhongshan, Beijing, China). Antibody-antigen complexes were detected using a chemiluminescent ECL reagent (Millipore).

2.6. Dual luciferase reporter gene construct and dual luciferase reporter assay

An 83 bp fragment of the Klf17 3′UTR containing the predicted binding site for hsa-miR-9 and flanking sequence on each side was synthetized with a short extension containing cleavage sites for XbaI (5′ end) and NotI (3′ end) (Suppl. Table 2); a second fragment containing a mutated sequence of the binding site was also synthesized. The two constructs were termed WT (Klf17-wild type) and MT (Klf17-mutant). The fragments were cloned into the pRL-TK vector (Promega Corporation, Madison, WI) downstream of the renilla luciferase reporter gene. The sequence of the miR-9 binding site and mutant site are shown in Suppl. Table 2. Each vector, along with 100 ng of pGL3 and 200 nmol/L miR-9 mimic or mimic control, was transfected into 293T cells using Lipofectamine 2000 (Invitrogen, Carlsbad, CA) according to the manufacturer's instructions. Cells were harvested 24 h after transfection and assayed for renilla and firefly luciferase activity using the Dual-Luciferase Reporter Assay System (Promega, Madison, WI, USA).

2.7. Chromatin immunoprecipitation (ChIP) assay

Chromatin immunoprecipitation (ChIP) was performed as previously described (Zhu et al., 2009). Antibodies used in this experiment were anti-KLF17 rabbit antibody (Sigma, St Louis, USA) and normal rabbit IgG (Sigma, St Louis, USA). The DNA isolated from the pull-down was subjected to PCR amplification using primers flanking the KLF17 binding site at the gene promoter (Suppl. Table 3). The PCR products were separated on a 2% agarose gel and stained with ethidium bromide.

2.8. In vitro cell proliferation assay

HepG2 and SMMC7721 cells transfected with the miR-9 mimic and NC mimic were detached with trypsin and seeded in 96-well plates (5×10^3/well). Cell proliferation was detected by CellTiter 96® AQueous (Promega, Madison, WI, USA) every 24 h.

2.9. In vitro cell cycle assay

HepG2 cells transfected with the miR-9 mimic, mimic control were cultured for 3 days, then harvested and quantified. One million tumor cells were fixed with 70% cold ethanol at 4 °C for 30 min, washed with PBS twice, and stained with 50 μg/ml PI (Sigma, USA) at room temperature for 5 min. Data was analyzed with ModFIT software.

2.10. In vitro migration and invasion assay

Transwell chambers (8-uM pore size; Costar) were used in the in vitro migration assay. HCC cells were transfected with the miR-9 mimic or the mimic control. After 48 h, cells were detached with trypsin, washed with PBS and resuspended in serum-free medium. Two hundred microliters of cell suspension (1×10^6 cells/ml of HepG2 or SMMC7721, 5×10^5 cells/ml of Hep11 or Hep12) was added to the upper chamber, and 500 μl of complete medium was added to the bottom well. The cells that had not migrated were removed from the upper surfaces of the filters using cotton swabs, and the cells that had migrated to the lower surfaces of the filters were fixed with 4% Paraformaldehyde solution and stained with Crystal Violet. Images of three random fields (10× magnification) were captured from each membrane, and the number of migratory cells was counted. Similar inserts coated with Matrigel were used to determine the invasive potential.

2.11. Lentiviral vector preparation and transduction

miR-9 and a negative control expression cassette were first constructed in pcDNA™6.2-GW/EmGFPmiR vector (Invitrogen, Catalog no. K4936-00). The inserted oligosequences were designed by Invitrogen and are listed in Suppl. Table 4. The miRNA expressing cassettes were then constructed in pLenti6/BLOCK-iT™-DEST vector by recombination. Lentiviral stock was produced by concentrating the supernatant harvested from 293T cells that were co-transfected with pLenti6/BLOCK-iT™-DEST and the packaging mix.

Lentivirus production and HepG2 transduction were performed as previously described (Zamule et al., 2008). HepG2 cells that overexpressed miR-9 and the control cells were named HepG2-miR-9 and HepG2-NC, respectively. Successfully transduced HepG2 cells were selected in culture media containing Blasticidin (Invitrogen, R210-01, 8 μg/ml) 24 h after transduction. The transduction efficiency was evaluated by detecting GFP expression under a fluorescence microscope, and the miR-9 expression level was determined by qRT-PCR 2 weeks after selection.

2.12. *Evaluation of metastasis regulation by miR-9 in mice*

Six- to eight-week-old male nude mice (BALB/c-nu) were purchased from the Experimental Animal Institute of the Chinese Academy of Medical Sciences (Beijing, China). The mice were bred and maintained under defined flora conditions in individually ventilated (high-efficiency particle-arresting filtered air) sterile microisolator cages (Techniplast, Milan, Italy). All animal handling and experimental procedures were approved by the Animal Care and Use Committee of the Chinese Academy of Medical Sciences. HepG2-miR-9 and HepG2-NC cells were prepared (5×10^6 cells in 200 μl PBS) and inoculated subcutaneously into the abdominal area. Tumor growth measurement and histological evaluation of tumor masses were performed on these two groups of mice (HepG2-miR-9 and HepG2-NC) every 2 weeks. Liver tissues were fixed in 10% neutral buffered formalin and paraffin-embedded. Three non-adjacent serial sections were hematoxylin and eosin stained. Metastatic index, the average metastases per unit area of liver averaged for miR-9 group and compare to the control group (NC group) by the non-parametric Mann–Whitney *U* test to determine statistical significance (Yang et al., 2004).

3. Results

3.1. *Hep12 is a highly metastatic cell line*

Using the transwell assay, we compared the invasion and migration capacity of Hep11 and Hep12 cells in vitro, and confirmed that Hep12 had a higher invasive and migratory potential than Hep11 (Figure 1A). Because EMT has been previously identified as an essential step in tumor cell invasion and migration, we measured the expression levels of EMT-related genes with qRT-PCR (Beltran et al., 2008; Komatsu et al., 2008; Hsu et al., 2009; Lundgren et al., 2009; Pena et al., 2009). As expected, Hep12 expressed more Sip, MBP, Snail 1 and HNRNPK than Hep11 (Figure 1B). Furthermore, we performed a comprehensive human specific miRNA microarray analysis to detect differences in miRNA expression between Hep11 and Hep12 cells. There were 156 miRNAs with significantly different expression levels between the two cell lines. Of these miRNAs, 139 have at least two folds different expression levels (95 were upregulated and 44 were downregulated in Hep12). (Figure 1C, Suppl. Table 4). The most differentially expressed miRNA was miR-9, whose expression in Hep12 was 1000-fold greater than that in Hep11. Because many studies have already reported miR-9 as an oncogene-like miRNA, to better understand its function in HCC, we used qRT-PCR to examine the expression of miR-9 in Hep11, Hep12 and two other cell lines (HepG2 and SMMC7721) with low invasive potential (Xue et al., 2007; Li et al., 2011a,b). Hep12 had a 184-fold higher expression of miR-9 than Hep11, whereas Hep11, HepG2 and SMMC7721 all had similar levels of miR-9 expression (Figure 1D).

3.2. *miR-9 promoted migration and invasion of HCC cell lines in vitro*

We further investigated the effect of miR-9 on the migration and invasion of hepatocellular carcinoma cells (HCC). Hep11, HepG2 and SMMC7721 all had similar low levels of miR-9 expression, so we transfected these cells with either the miR-9 mimic or the mimic control (the efficiency of transfection shown in Suppl. Figure 1) The transfected cells were then subjected to cell migration assay and cell invasion assay for 24 h and 72 h, respectively. Cell motility in all cell lines was significantly enhanced after transfection of the miR-9 mimic

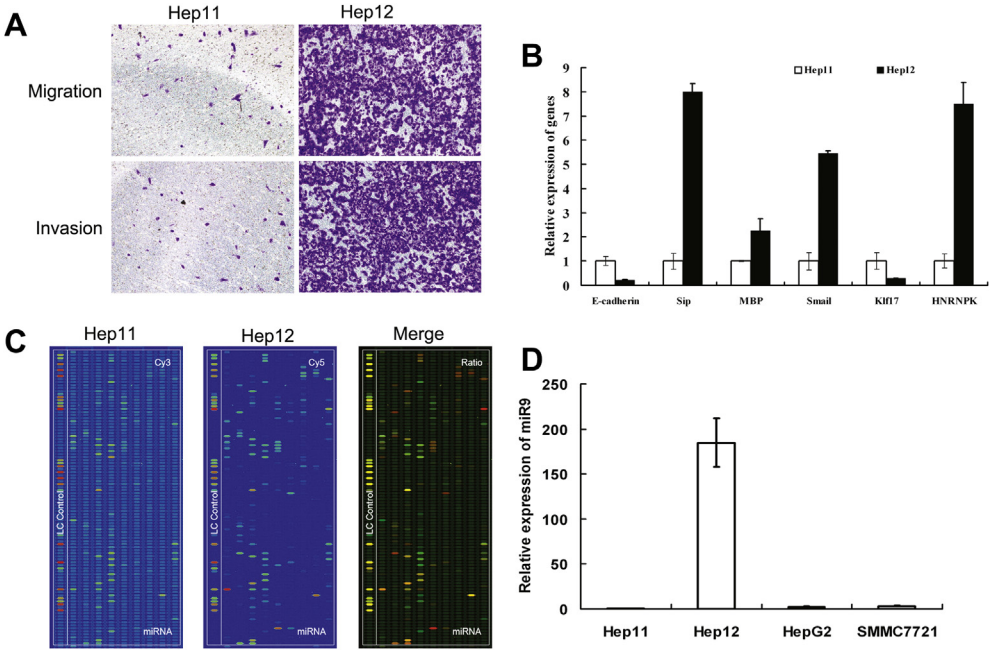

Figure 1 – Comparison of Hep11 and Hep12 characteristics. (A) Transwell migration ($n = 3$) and invasion ($n = 3$) assays showed that Hep12 had greater migratory and invasive potentials than Hep11. (B) Relative expression of EMT-related genes. (C) The microRNA microarray analysis of Hep11 and Hep12. (D) Expression of miR-9 in Hep11, Hep12, HepG2 and SMMC7721 cells by real time PCR.

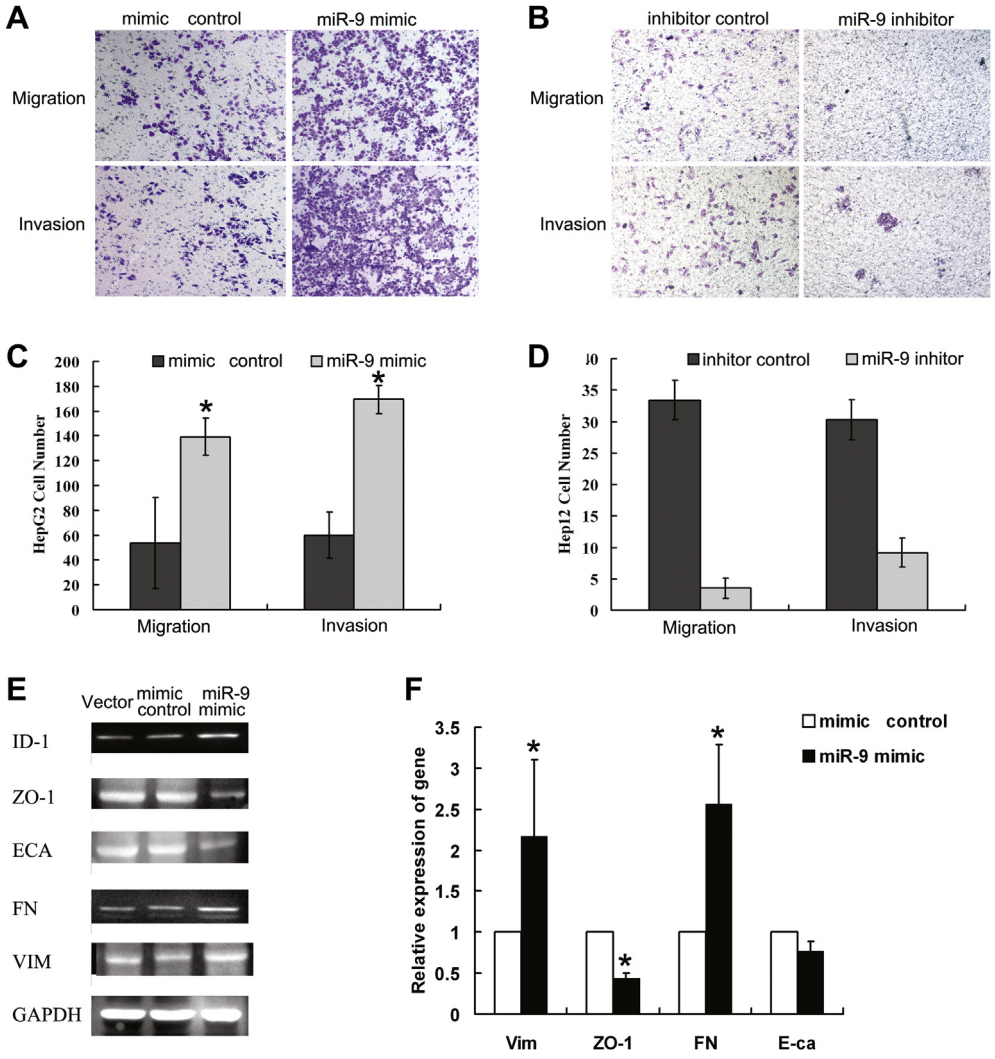

Figure 2 – miR-9 regulated hepatocellular carcinoma cell migration and invasion. (A, C) Transwell migration ($n = 4$) and invasion ($n = 4$) assays showed that HepG2 cells transfected with the miR-9 mimic (800 nM) had greater invasive and migratory potentials than the control (mimic control). (A) is a microscopic image of Crystal violet staining; (C) shows the statistical results. Data represent the mean ± SD of four independent experiments. *$P < 0.01$. (B, D) Transwell migration ($n = 4$) and invasion ($n = 4$) assays showed that Hep12 cells transfected with the miR-9 inhibitor (800 nM) had lower invasive and migratory potentials than the control (inhibitor control). (B) is a microscopic image of Crystal violet staining; (D) shows the statistical results. Data represent the mean ± SD of four independent experiments. *$P < 0.01$. Western blot (E) and real time PCR (F) showed that epithelial markers were downregulated and mesenchymal markers were up-regulated in HepG2 cells transfected with the miR-9 mimic (800 nM). Vector: untreated cells; mimic control: cells transfected with the mimic control; miR-9 mimic: cells transfected with the miR-9 mimic.

(Figure 2A,C and Suppl. Figure 2 and 3). On the other hand, Hep12 cells were transfected with the miR-9 inhibitor or the inhibitor control (the efficiency of transfection shown in Suppl. Figure 4) and subjected to the migration assay and the invasion assay for 8 h and 24 h, respectively. Hep12 migration and invasion were significantly reduced after miR-9 inhibitor transfection compared with the inhibitor control (Figure 2B,D). Interestingly, miR-9 had no effect on the proliferation of HepG2 (Suppl. Figure 5A) and SMMC7721 (Suppl. Figure 5B) cells. miR-9 also had no impact on the cell cycle profile of HepG2 cells (Suppl. Figure 5C). The mechanism by which miR-9 affects the motility of HCC may lie in its regulation of EMT. Therefore, we assessed the RNA and protein expression levels of epithelia- and mesenchyme-related genes in HepG2 and SMMC7721 cells that were transfected with the miR-9 mimic or the mimic control for 48 h. We demonstrated that the epithelial markers E-cadherin and ZO-1 were downregulated and that the mesenchymal markers, including VIMENTIN, ID-1 and FN, were up-regulated in HepG2 and SMMC7721 cells that were transfected with the miR-9 mimic compared with cells transfected with the mimic control (Figure 2E,F and Suppl. Figure 6).

3.3. *miR-9 directly inhibited KLF17 expression via its 3′UTR*

Bioinformatics analysis suggested that there was a conservative binding site of miR-9 in the Klf17 3′UTR (Figure 3A). To test

this hypothesis, we conducted a standard luciferase reporter assay in 293T cells. The cells were transfected with the luciferase construct Klf17-WT or Klf17-MT, along with the internal control vector pGL3 and either the miR-9 mimic or the mimic control. The cells were harvested at 48 h and analyzed for dual luciferase activity. The results showed that the renilla luciferase activity in Klf17-WT-transfected cells decreased by more than 40% in miR-9 mimic-cotransfected cells compared with that in mimic control-cotransfected cells. In addition, site-directed mutagenesis of the seed region offset the inhibitory effect of miR-9 mimic (Figure 3B).

To determine whether miR-9 could regulate the expression of KLF17 in HCC, we measured the RNA and protein levels of KLF17 in HepG2 cells that were transfected with the miR-9 mimic or the mimic control and in Hep12 cells that were transfected with the miR-9 inhibitor or the inhibitor control. The results showed that expression of Klf17 remained unchanged at the mRNA level (Figure 3C), but the KLF17 protein level was reduced in HepG2 and Hep11 cells after transfection with the miR-9 mimic (Figure 3D,F), and the protein level was increased in Hep12 cells after transfection with the miR-9 inhibitor (Figure 3E).

3.4. *KLF17 downregulated migration and invasion of hepatocellular carcinoma cells*

To analyze the function of KLF17 in HCC, we transfected HepG2 with siRNA of KLF17 and evaluated its effect on EMT-related markers. In comparison with cells transfected with an siRNA control (Si-control), the epithelial markers E-cadherin and ZO-1 were downregulated and the mesenchymal markers VIMENTIN, ID-1 and FIBRONECTIN were upregulated in cells transfected with Klf17 siRNA (Figure 4A,B). We further investigated the effect of KLF17 on the migration and invasion of HCC. HepG2 and SMMC7721 cells were transfected with either the Klf17 siRNA or the Si-control, and then cell migration and invasion were evaluated (Figure 4C,D,E,F). We observed that cell motility was significantly enhanced after KLF17 knockdown relative to the control.

3.5. *ZO-1, Vimentin and FN were directly regulated by KLF17*

It has been shown that the transcription factor KLF17 binds to the DNA consensus sequence 5′-CACCC-3′ and plays a role in transcriptional regulation. Id-1 was reported to be directly regulated by KLF17. Bioinformatics analysis indicated that KLF17 binding sites also existed in the promoter regions of ZO-1, Vimentin, Fibronectin and β-catenin. To identify the downstream gene targets regulated by KLF17, we performed ChIP assays and found that KLF17 could bind directly to the promoter regions of ZO-1 (−1913/-1909; −1540/−1536), Vimentin (−280/−276) and Fibronectin (−995/−991) (Figure 5).

3.6. *miR-9 promoted metastasis in mice*

To further characterize the effects of miR-9 on HCC in vivo, we constructed HepG2 cells with stable overexpression of miR-9

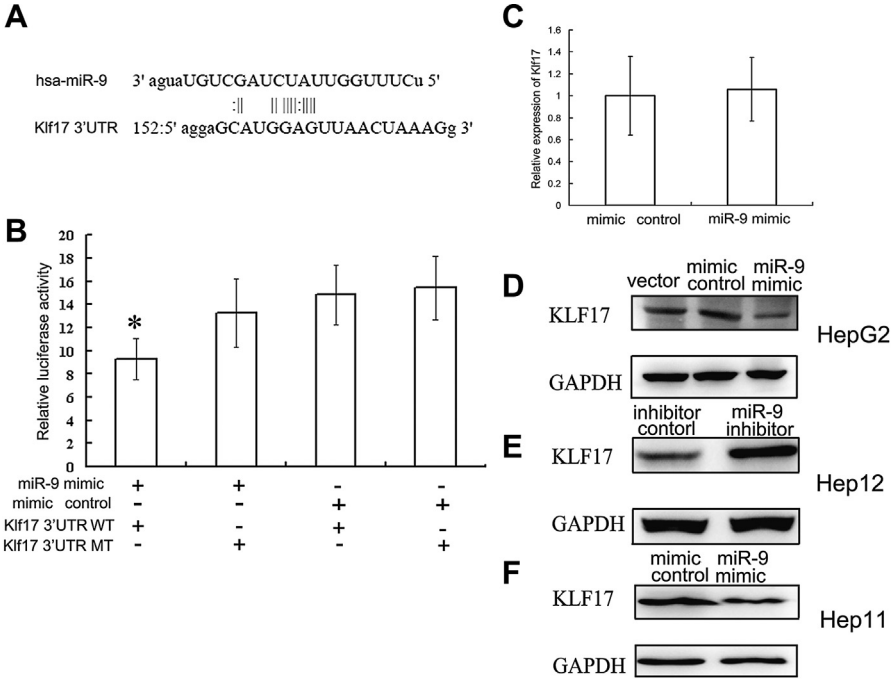

Figure 3 – Klf17 was a direct target of miR-9. (A) Analysis of the Klf17 3′UTR sequence by TargetScan revealed a putative miR-9 binding site. (B) The miR-9 binding site on Klf17 3′UTR was confirmed by luciferase assay in 293T cells after cotransfection with (i) a plasmid containing a fragment of Klf17 3′UTR that included either the wild type or mutant predicted miR-9 binding site and (ii) the miR-9 mimic or the mimic control. Data represent the mean ± SD of at least three independent experiments. *$P < 0.01$. (C) Real time PCR showed that miR-9 did not affect Klf17 mRNA expression. (D) Western blot assay showed increased KLF17 expression in HepG2 cells after transfection with the miR-9 mimic (800 nM). Western blot assay showed KLF17 expression in Hep12 cells transfected with the miR-9 inhibitor (E) and Hep11 cells transfected with the miR-9 mimics (F).

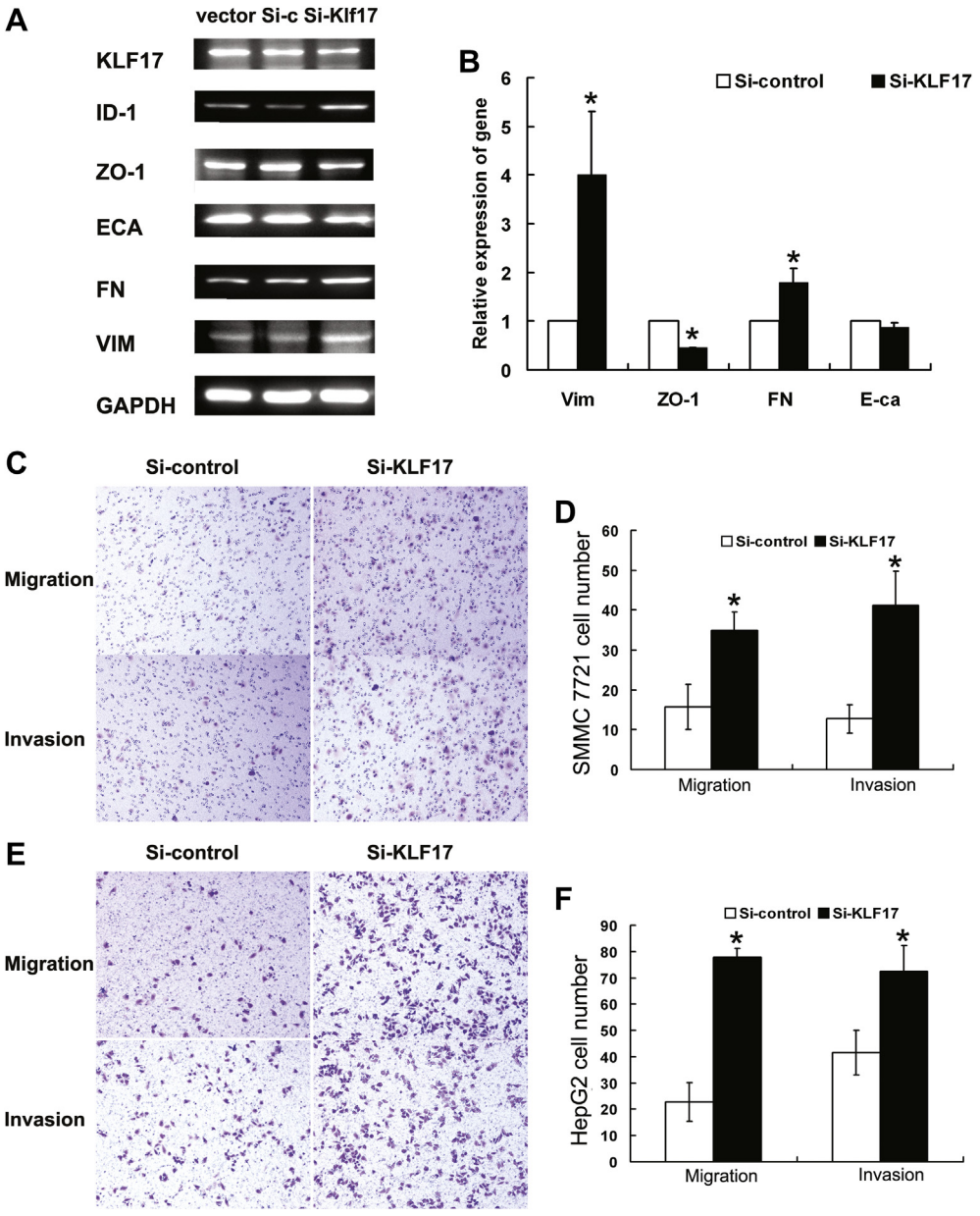

Figure 4 – KLF17 regulated hepatocellular carcinoma cell migration and invasion. (A) Western blot assay showed that epithelial markers were downregulated and mesenchymal markers were up-regulated in HepG2 cells transfected with the miR-9 mimic (800 nM). (B) Real time PCR showed that epithelial markers were downregulated and mesenchymal markers were up-regulated in HepG2 cells transfected with the Klf17 siRNA (200 nM). (C, D) Transwell migration ($n = 4$) and invasion ($n = 4$) assays showed that SMMC7721 cells that were transfected with the Klf17 siRNA (200 nM) had greater invasive and migratory potentials than the control (siRNA control). (C) is a microscopic image of Crystal violet staining; (D) shows the statistical results. Data represent the mean ± SD of four independent experiments. *$P < 0.01$. (E, F) Transwell migration ($n = 4$) and invasion ($n = 4$) assays showed that HepG2 cells that were transfected with Klf17 siRNA (200 nM) had greater invasive and migratory potentials than the control (siRNA control). (E) is the microscopic image of Crystal violet staining; (F) shows the statistical results. Data represent the mean ± SD of four independent experiments. *P < 0.01. Vector: untreated cells; Si-c (Si-control): cells transfected with the siRNA control; Si-KLF17: cells transfected with the KLF17 siRNA.

(HepG2-miR-9) and the respective control cells (HepG2-NC) through lentiviral vector delivery (The efficiency of transfection is shown in Figure 6A). These cells were injected subcutaneously into nude mice. Tumor masses were measured every 2 weeks, and mice from the two groups (HepG2-miR-9 and HepG2-NC) were also sacrificed every 2 weeks to detect any development of liver metastasis. Our results showed that there was no significant difference in tumor size between the two groups (Figure 6B,C). However, no liver metastasis occurred as early as 4 weeks after injecting mice with HepG2-miR-9 cells at the two groups (data not shown), but multiple metastatic masses were detected after 8 weeks in miR-9 groups. In comparison, fewer metastases arose after 8 weeks in the control group (Figure 6D,E). Metastatic index of

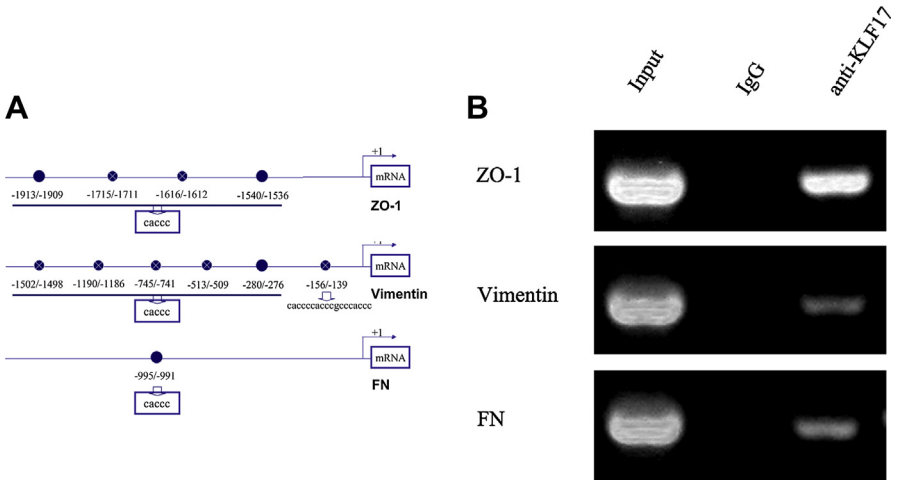

Figure 5 – Expression of ZO-1, Vimentin and FN in hepatocellular carcinoma cells was regulated by KLF17. (A) The putative KLF17 binding sites (caccc) in three gene promoter regions. (B) Chromatin immunoprecipitation (ChIP) was performed using an anti-KLF17 antibody and a rabbit IgG as the control. The ZO-1, Vimentin and FN promoter region where KLF17 binds showed significant enrichment after immunoprecipitation by an anti-KLF17 antibody.

the control group, as measured by the density of tumor lesions per area of liver tissue scored in non-adjacent serial sections, the MI of miR-9 over-expression were 44.81 ± 20.76 (compare to control group, $P < 0.05$) (Figure 6F). These data showed tht miR-9 may promote metastasis in HCC. No obvious lung metastasis was observed in either group.

4. Discussion

Like other microRNAs, whether miR-9 acts as a tumor suppressor or oncogene in different types of tumors is still an unfolding controversy. Due to a disparity of target binding sites, miR-9 plays opposite roles in the development and progression of different tumors. It inhibits tumor proliferation and migration in melanoma (Liu et al., 2012) and ovarian cancer (Guo et al., 2009). In contrast, it enhances tumor proliferation and invasion in head and neck squamous cell carcinoma (HNSCC) (Luo et al., 2012), breast cancer (Zhou et al., 2012), gastric cancer (Rotkrua et al., 2011) and colon cancer (Zhu et al., 2012). Ma L et al. reported that miR-9 is induced by Myc in breast cancer cells, where it targets the major epithelial adherens junction protein E-cadherin. MiR-9-mediated E-cadherin downregulation primes the cancer cells for EMT and also stimulates angiogenesis in tumors (Ma et al., 2010).

HCC recurrence may originate from intrahepatic metastasis or independent multicentric manifestation. In HBV-associated HCC, the origin of recurrence can be determined by analyzing the integration sites of HBV DNA. Hep11 and Hep12 cells have the same HBV integration site, suggesting that they may have the same clonal origin, as previously described (Xu et al., 2010a,b). Therefore, Hep12 may have arisen from micro-intrahepatic metastases of Hep11.

We first compared the metastatic capacity and EMT-related gene expression of Hep11 and Hep12. Our results suggest that Hep12 cells possess mesenchymal characteristics with higher expression of EMT-related genes and an enhanced invasive ability compared with Hep11 cells. To investigate whether these discrepancies between Hep11 and Hep12 could be explained by distinct microRNA expression, we performed microRNA microarray profiling in the two cell lines. As expected, 156 miRNAs with significantly different expression levels were detected. The most differentially expressed miRNA was miR-9, whose expression in Hep12 was 1000-fold greater than that in Hep11. This result was also confirmed by qRT-PCR. Does higher expression of miR-9 in Hep12 contribute to its higher migratory capacity? To test this hypothesis, we performed in vitro functional assays after transfecting miR-9 mimic into HepG2 and SMMC7721 cells, two cell lines with similar levels of endogenous miR-9 as Hep11 and lower metastatic potential than Hep12. We found that miR-9 overexpression promoted migration and invasion in these cells. Concurrently, miR-9 overexpression also caused down-regulation of epithelial marker expression and up-regulation of mesenchymal marker expression, indicating that overexpression of miR-9 might promote EMT in HCC.

MicroRNAs are small non-coding RNA molecules that affect gene expression regulation by acting as post-transcriptional regulators. According to the prediction of microRNA.org, Klf17 might be a target gene of miR-9. KLF17 has already been reported to be a negative regulator of EMT and metastasis in breast cancer (Gumireddy et al., 2009), and lung adenocarcinoma (Cai et al., 2012). It has reported that reduced expression of KLF17 promoted motility and invasion ability of HepG2 cells and changed the expression of E-cadherin, ZO-1, Snail, and vimentin (Liu et al., 2013). Our study bridged the gap between higher miR-9 expression and lower KLF17 expression in Hep12 cells by demonstrating that KLF17 was a direct target of miR-9. Firstly the luciferase reporter assay showed that miR-9 could bind to the 3′UTR of Klf17 and suppress its expression. Secondly, up-regulation of miR-9 by miR-9 mimic transfection in miR-9 low expression HCC cell lines led to downregulation of KLF17 protein expression while down-regulation of the miR-9 by miR-9 inhibitors

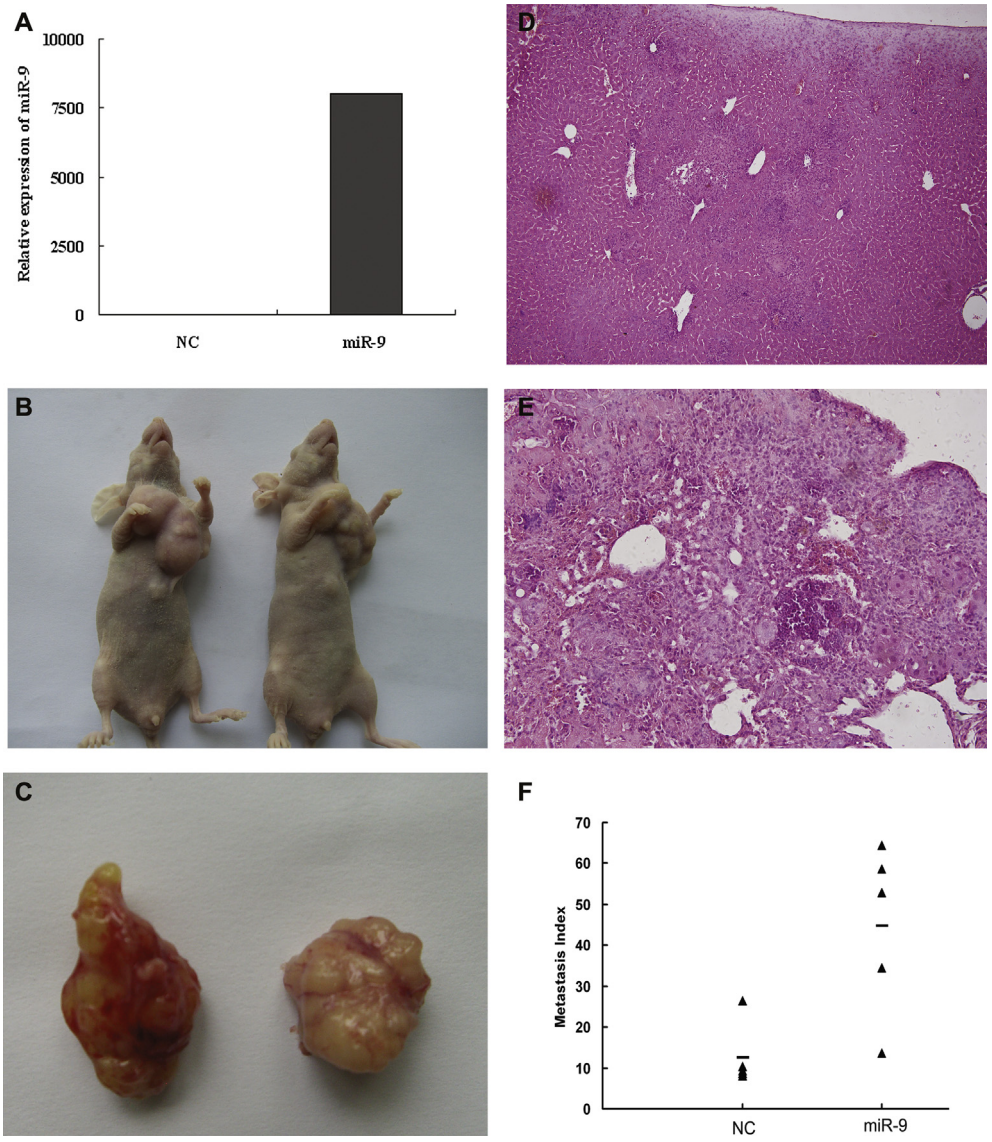

Figure 6 – miR-9 suppressed tumor metastasis in vivo. (A) Real time PCR analysis of the lentiviral vector transduction efficiency in HepG2 cells. (B) The mice were transplanted with hepatocellular carcinoma cells (Left, HepG2 transfected with control; Right, HepG2 transfected with miR-9) by subcutaneous injection (8 weeks). (C) The primary tumors (8 weeks). (D,E) Pathological images of liver metastases (8 weeks). D, HepG2 transfected control; E, HepG2 transfected with miR-9. (F) Metastasis index (MI) of NC and miR-9 group, ▲ is MI of one section;– is the mean.

in higher miR-9 expression Hep12 cells resulted in increased KLF17 protein expression.

How KLF17 regulate HCC migration and invasion? It was reported that KLF17 could act as a key negative regulator of EMT via inhibition of Id1 transcription by directly binding to its promoter region (Gumireddy et al., 2009). Here, we provide more evidence to the molecular mechanisms governing the regulation of EMT by KLF17. According to a transcription factor binding motif analysis, the gene promoters of ZO-1, Fibronectin, beta-catenin and Vimentin also contain predicted KLF17 binding sites. Our KLF17-ChIP results showed that KLF17 bound to the promoter regions of Fibronectin, ZO-1 and Vimentin but not to that of beta-catenin, suggesting that KLF17 might directly regulate other EMT-related genes in addition to Id-1. In summary, these findings demonstrate that miR-9 promoted HCC metastasis through the indirect regulation of EMT-related genes, such as Fibronectin, ZO-1 and Vimentin, as a consequence of its direct post-transcriptional inhibition of KLF17.

5. Conclusion

Our results have demonstrated that overexpression of miR-9 and suppression of KLF17 could be used as predictive markers of high metastatic potential in HCC. We also propose that the miR-9-KLF17 signaling pathway might act as a potential therapeutic target in HCC.

Conflict of interest

No.

Acknowledgments

Supported by grants from the National Natural Science Foundation of China (No. 81101588, 30800429, 30911130363); "863 Projects" of Ministry of Science and Technology of PR China (No. 2011AA020100); The National Key Scientific Program of China (No. 2011CB964901); and the Program for Changjiang Scholars and Innovative Research Team in University-PCSIRT (No. IRT0909)

Appendix A. Supplementary data

Supplementary data related to this article can be found at http://dx.doi.org/10.1016/j.molonc.2013.04.007.

REFERENCES

Beltran, M., Puig, I., Pena, C., Garcia, J.M., Alvarez, A.B., Pena, R., Bonilla, F., de Herreros, A.G., 2008. A natural antisense transcript regulates Zeb2/Sip1 gene expression during Snail1-induced epithelial-mesenchymal transition. Genes Dev. 22, 756–769.

Budhu, A., Jia, H.L., Forgues, M., Liu, C.G., Goldstein, D., Lam, A., Zanetti, K.A., Ye, Q.H., Qin, L.X., Croce, C.M., Tang, Z.Y., Wang, X.W., 2008. Identification of metastasis-related microRNAs in hepatocellular carcinoma. Hepatology 47, 897–907.

Cai, X.D., Zhou, Y.B., Huang, L.X., Zeng, Q.L., Zhang, L.J., Wang, Q.Q., Li, S.L., Feng, J.Q., Han, A.J., 2012. Reduced expression of Kruppel-like factor 17 is related to tumor growth and poor prognosis in lung adenocarcinoma. Biochem. Biophys. Res. Commun. 418, 67–73.

Ferlay, J., Shin, H.R., Bray, F., Forman, D., Mathers, C., Parkin, D.M., 2010. Estimates of worldwide burden of cancer in 2008: GLOBOCAN 2008. Int. J. Cancer 127, 2893–2917.

Gumireddy, K., Li, A., Gimotty, P.A., Klein-Szanto, A.J., Showe, L.C., Katsaros, D., Coukos, G., Zhang, L., Huang, Q., 2009. KLF17 is a negative regulator of epithelial-mesenchymal transition and metastasis in breast cancer. Nat. Cell. Biol. 11, 1297–1304.

Guo, L.M., Pu, Y., Han, Z., Liu, T., Li, Y.X., Liu, M., Li, X., Tang, H., 2009. MicroRNA-9 inhibits ovarian cancer cell growth through regulation of NF-kappaB1. FEBS J. 276, 5537–5546.

Hsu, K.W., Hsieh, R.H., Wu, C.W., Chi, C.W., Lee, Y.H., Kuo, M.L., Wu, K.J., Yeh, T.S., 2009. MBP-1 suppresses growth and metastasis of gastric cancer cells through COX-2. Mol. Biol. Cell. 20, 5127–5137.

Jemal, A., Bray, F., Center, M.M., Ferlay, J., Ward, E., Forman, D., 2011. Global cancer statistics. CA Cancer J. Clin. 61, 69–90.

Komatsu, H., Fujimoto, S., Hara, S., Sato, Y., Yamada, K., Kitamura, K., 2008. Effect of tonsillectomy plus steroid pulse therapy on clinical remission of IgA nephropathy: a controlled study. Clin. J. Am. Soc. Nephrol. 3, 1301–1307.

Li, Y., Guo, J., Wang, C., Fan, Z., Liu, G., Wang, C., Gu, Z., Damm, D., Mosig, A., Wei, X., 2011a. Circulation times of prostate cancer and hepatocellular carcinoma cells by in vivo flow cytometry. Cytometry A 79, 848–854.

Li, Z.Y., Xi, Y., Zhu, W.N., Zeng, C., Zhang, Z.Q., Guo, Z.C., Hao, D.L., Liu, G., Feng, L., Chen, H.Z., Chen, F., Lv, X., Liu, D.P., Liang, C.C., 2011b. Positive regulation of hepatic miR-122 expression by HNF4alpha. J. Hepatol. 55, 602–611.

Lin, Z.S., Chu, H.C., Yen, Y.C., Lewis, B.C., Chen, Y.W., 2012. Kruppel-like factor 4, a tumor suppressor in hepatocellular carcinoma cells reverts epithelial mesenchymal transition by suppressing slug expression. PLoS One 7, e43593.

Liu, F.Y., Deng, Y.L., Li, Y., Zeng, D., Zhou, Z.Z., Tian, D.A., Liu, M., 2013. Down-regulated KLF17 expression is associated with tumor invasion and poor prognosis in hepatocellular carcinoma. Med. Oncol. 30, 425.

Liu, S., Kumar, S.M., Lu, H., Liu, A., Yang, R., Pushparajan, A., Guo, W., Xu, X., 2012. MicroRNA-9 up-regulates E-cadherin through inhibition of NF-kappaB1-Snail1 pathway in melanoma. J. Pathol. 226, 61–72.

Lundgren, K., Nordenskjold, B., Landberg, G., 2009. Hypoxia, Snail and incomplete epithelial-mesenchymal transition in breast cancer. Br. J. Cancer 101, 1769–1781.

Luo, X., Fan, S., Huang, W., Zhai, S., Ma, Z., Li, P., Sun, S.Y., Wang, X., 2012. Downregulation of IRS-1 promotes metastasis of head and neck squamous cell carcinoma. Oncol. Rep. 28, 659–667.

Ma, L., Young, J., Prabhala, H., Pan, E., Mestdagh, P., Muth, D., Teruya-Feldstein, J., Reinhardt, F., Onder, T.T., Valastyan, S., Westermann, F., Speleman, F., Vandesompele, J., Weinberg, R.A., 2010. miR-9, a MYC/MYCN-activated microRNA, regulates E-cadherin and cancer metastasis. Nat. Cell. Biol. 12, 247–256.

Oishi, N., Kumar, M.R., Roessler, S., Ji, J., Forgues, M., Budhu, A., Zhao, X., Andersen, J.B., Ye, Q.H., Jia, H.L., Qin, L.X., Yamashita, T., Goo, W.H., Jun, K.Y., Kaneko, S., Tang, Z.Y., Thorgeirsson, S.S., Wei, W.X., 2012. Transcriptomic profiling reveals hepatic stem-like gene signatures and interplay of miR-200c and epithelial-mesenchymal transition in intrahepatic cholangiocarcinoma. Hepatology 56, 1792–1803.

Pena, C., Garcia, J.M., Larriba, M.J., Barderas, R., Gomez, I., Herrera, M., Garcia, V., Silva, J., Dominguez, G., Rodriguez, R., Cuevas, J., de Herreros, A.G., Casal, J.I., Munoz, A., Bonilla, F., 2009. SNAI1 expression in colon cancer related with CDH1 and VDR downregulation in normal adjacent tissue. Oncogene 28, 4375–4385.

Rotkrua, P., Akiyama, Y., Hashimoto, Y., Otsubo, T., Yuasa, Y., 2011. MiR-9 downregulates CDX2 expression in gastric cancer cells. Int. J. Cancer 129, 2611–2620.

Tan, H.X., Wang, Q., Chen, L.Z., Huang, X.H., Chen, J.S., Fu, X.H., Cao, L.Q., Chen, X.L., Li, W., Zhang, L.J., 2010. MicroRNA-9 reduces cell invasion and E-cadherin secretion in SK-Hep-1 cell. Med. Oncol. 27, 654–660.

Wen, W., Ding, J., Sun, W., Fu, J., Chen, Y., Wu, K., Ning, B., Han, T., Huang, L., Chen, C., Xie, D., Li, Z., Feng, G., Wu, M., Xie, W., Wang, H., 2012. Cyclin G1-mediated epithelial-mesenchymal transition via phosphoinositide 3-kinase/Akt signaling facilitates liver cancer progression. Hepatology 55, 1787–1798.

Xu, X.L., Xing, B.C., Han, H.B., Zhao, W., Hu, M.H., Xu, Z.L., Li, J.Y., Xie, Y., Gu, J., Wang, Y., Zhang, Z.Q., 2010a. The properties of tumor-initiating cells from a hepatocellular carcinoma patient's primary and recurrent tumor. Carcinogenesis 31, 167–174.

Xu, X., Xing, B., Hu, M., Xu, Z., Xie, Y., Dai, G., Gu, J., Wang, Y., Zhang, Z., 2010b. Recurrent hepatocellular carcinoma cells with stem cell-like properties: possible targets for immunotherapy. Cytotherapy 12, 190–200.

Xue, T.C., Chen, R.X., Ye, S.L., Sun, R.X., Chen, J., Tang, Z.Y., 2007. Different expressions of chemokine receptors in human hepatocellular carcinoma cell lines with different metastatic potentials. Zhonghua Gan Zang Bing Za Zhi 15, 261–265.

Yang, H., Rouse, J., Lukes, L., Lancaster, M., Veenstra, T., Zhou, M., Shi, Y., Park, Y.G., Hunter, K., 2004. Caffeine suppresses metastasis in a transgenic mouse model: a prototype molecule for prophylaxis of metastasis. Clin. Exp. Metastasis 21, 719–735.

Zamule, S.M., Strom, S.C., Omiecinski, C.J., 2008. Preservation of hepatic phenotype in lentiviral-transduced primary human hepatocytes. Chem. Biol. Interact. 173, 179–186.

Zhou, X., Marian, C., Makambi, K.H., Kosti, O., Kallakury, B.V., Loffredo, C.A., Zheng, Y.L., 2012. MicroRNA-9 as potential biomarker for breast cancer local recurrence and tumor estrogen receptor status. PLoS One 7, e39011.

Zhu, L., Chen, H., Zhou, D., Li, D., Bai, R., Zheng, S., Ge, W., 2012. MicroRNA-9 up-regulation is involved in colorectal cancer metastasis via promoting cell motility. Med. Oncol. 29, 1037–1043.

Zhu, Y., Sun, Z., Han, Q., Liao, L., Wang, J., Bian, C., Li, J., Yan, X., Liu, Y., Shao, C., Zhao, R.C., 2009. Human mesenchymal stem cells inhibit cancer cell proliferation by secreting DKK-1. Leukemia 23, 925–933.